

BRIEF REPORT

Open Access



Age-related cerebral ventriculomegaly occurs in patients with primary ciliary dyskinesia

Franziska Eisenhuth¹, Joy E. Agbonze², Adam M. R. Groh^{3,4}, Jesse M. Klostranec^{5,6}, David A. Rudko^{3,4,7}, Jo Anne Stratton^{4,9*†} and Adam J. Shapiro^{2,8*†}

Abstract

Primary ciliary dyskinesia (PCD) is a genetic disorder causing motile ciliary dysfunction primarily affecting the respiratory and reproductive systems. However, the impact of PCD on the central nervous system remains poorly understood. Rodent models of PCD exhibit marked hydrocephalus leading to early animal mortality, however, most humans with PCD do not develop hydrocephalus for unknown reasons. We hypothesized that patients with PCD exhibit sub-clinical ventriculomegaly related to ependymal motile ciliary dysfunction. We demonstrated highly specific expression levels of known PCD-related genes in human brain multiciliated ependymal cells ($p < 0.0001$). To assess ventricular size, computed tomography sinus images from patients with PCD ($n = 33$) and age/sex-matched controls ($n = 64$) were analysed. Patients with PCD displayed significantly larger ventricular areas ($p < 0.0001$) and Evans index ($p < 0.01$), indicating ventriculomegaly that was consistent across all genetic subgroups. Ventricular enlargement correlated positively with increasing age in patients with PCD compared to controls ($p < 0.001$). Additionally, chart review demonstrated a high prevalence (39%) of neuropsychiatric/neurological disorders in adult PCD patients that did not correlate with degree of ventriculomegaly. Our findings suggest that patients with PCD may have unrecognized, mild ventriculomegaly which correlates with ageing, potentially attributable to ependymal ciliary dysfunction. Further study is required to determine causality, and whether ventricular enlargement contributes to neuropsychiatric/neurological or other morbidity in PCD.

Keywords Primary ciliary dyskinesia, Hydrocephalus, Ventriculomegaly, Lateral ventricles, CT, Neuropsychiatric illness

[†]Jo Anne Stratton and Adam J. Shapiro contributed equally to this work, co-corresponding.

*Correspondence:

Jo Anne Stratton
Jo.Stratton@mcgill.ca
Adam J. Shapiro
Adam.Shapiro.med@ssss.gouv.qc.ca

¹Michael G. DeGroote School of Medicine, McMaster University, Hamilton, ON L8S 4L8, Canada

²Research Institute of the McGill University Health Centre, Montreal, QC H4A 3J1, Canada

³Montreal Neurological Institute-Hospital, McGill University, Montreal, QC H3A 2B4, Canada

⁴Department of Neurology and Neurosurgery, McGill University, Montreal, QC H3A 1A1, Canada

⁵Department of Neuroradiology, Montreal Neurological Institute and Hospital, Montreal, QC H3A 2B4, Canada

⁶McGill University Health Centre, Montreal, QC H4A 3J1, Canada

⁷Department of Biomedical Engineering, McGill University, Montreal, QC H3A 2B4, Canada

⁸Montreal Children's Hospital, 1001 Decarie Blvd, Montreal, QC H4A 3J1, Canada

⁹Montreal Neurological Institute, 3801 University Drive, Montreal, QC H4A 3J1, Canada



Introduction

Primary ciliary dyskinesia (PCD) is a rare genetic disorder affecting motile ciliary function, with a prevalence of at least 1:7600 worldwide [1]. Variants in >50 unique genes result in disease-causing, ciliary ultrastructural defects, including outer dynein arm (ODA) defects, outer plus inner dynein arm (ODA + IDA) defects, IDA defects plus microtubule disorganization (IDA/MTD), central apparatus/radial spoke (CA/RSP) defects, or oligociliary defects with vast reductions in cilia number to only a few per cell [2]. In PCD, ciliary dysfunction usually affects respiratory cilia in the airways, nodal cilia in the left-right organizer of developing embryos, and reproductive cilia/flagellae. This dysfunction produces chronic cough and rhino-sinusitis, recurrent pneumonia with development of bronchiectasis, recurrent otitis media, left-right organ laterality defects, and subfertility.

The cerebral ventricles of the brain are lined with multiciliated ependymal cells where motile cilia beat in synchrony to aid in local circulation of cerebrospinal fluid (CSF) [3]. A preponderance of murine PCD models suggests disruption of ependymal ciliary function leads to hydrocephalus, a condition characterized by excessive accumulation of CSF in the cerebral ventricles. In knock out mouse models of PCD, variants in numerous different ciliary genes affect ependymal ciliary beating and appear to cause congenital hydrocephalus leading to early animal mortality [4–8]. Studies have also shown perturbed CSF flow as a direct result of ciliary defects. For example, the specific PCD-related genotype *HYDIN* (resulting in central apparatus defects) was initially discovered as a hydrocephalus causing defect in mice [9] and was later described in PCD-affected humans without hydrocephalus [10]. The pathology of hydrocephalic mice with *HYDIN* mutants seems to involve defects in CSF communication and absorption into the subarachnoid space, and edema in the extracellular space related to ciliary dysfunction. However, extensive phenotyping studies of large PCD patient populations do not show the development of hydrocephalus in humans [11–13], aside from rare cases with variants in genes affecting the NOTCH-1 signaling pathway, such as *CCNO* [14], *FOXJ1* [15], and *MCIDAS* [16]. The cause for this discrepancy between human and rodent studies is not clear.

With the pervasiveness of ependymal ciliary dysfunction and hydrocephalus in murine PCD models, we hypothesize that people with PCD may have unrecognized, subtle ventriculomegaly that could be related to ependymal ciliary dysfunction. The pathology by which ciliopathies could cause ventriculomegaly in humans is still unclear, however, multiple mechanisms, including those uncovered in mouse models (cellular edema or defects in bulk CSF flow, reduced clearance of CSF solutes, defects in pre- or post-natal neurologic

development) could be present [17–19]. While ventricular enlargement in patients with PCD may not present with clinical symptoms severe enough to warrant brain imaging, most patients undergo computed tomography (CT) of the head to evaluate chronic sino-nasal disease, providing a means to indirectly assess intracranial anatomy. We demonstrate that PCD-associated genes are exclusively expressed by human ependymal cells in the brain and provide the first evidence to suggest that there is broad ventricular enlargement in patients with PCD that correlates with age.

Materials and methods

Human brain donors underwent medical assistance in dying for various causes, including Multiple Sclerosis, Amyotrophic Lateral Sclerosis, or other (see Supplementary Table 1). Tissue samples ($n=7$) were obtained from the lateral horn of the lateral ventricle, adjacent to the caudate nucleus. As the cells in this dataset were from periventricular/ventricular wall whole brain tissue, there was no cell sorting. To remove debris from whole cells, tissue was first dissociated and then a density gradient was used. Cell suspensions were loaded into a 10x Chromium machine for GEM generation. Libraries were prepared per manufacturer's recommendations and subsequently sequenced. Fastq files were generated and used as input into the cellranger software, which generated filtered count matrices that were imported in R (v.4.2.3) using the Seurat (v4.3.0.1) package. Datasets were pre-processed, normalized and integrated using standard Seurat functions. PCA, UMAP, and gene expression calculations were also conducted using Seurat. A merged object of all periventricular datasets was used for analysis, and the transcriptomic profile of the ependymal cell cluster was defined by high expression of multiple cilia-associated genes such as *FOXJ1*, *PIFO*, *DYNLRB2*, and *CCDC153* [20, 21]. To determine the significance of average expression values for each PCD gene in ependymal cells compared to all other brain cell types, non-parametric Kruskal-Wallis tests and Dunn's multiple comparison's tests were conducted in GraphPad Prism (v8.0.1) using raw counts exported from R (Fig. 1).

We retrospectively obtained clinical CT head images (mainly for chronic sinusitis) in patients with PCD. All patients displayed chronic oto-sino-pulmonary infections as expected with PCD, but none had a clinical history of infections involving the central nervous system. A PCD diagnosis was confirmed through biallelic variants within one PCD gene and/or a classic ultrastructural defect on ciliary transmission electron microscopy (see Supplementary Table 2). Genetic analyses were performed through various commercial genetic panels investigating variants in >40 PCD-causing genes [22], but no additional analyses were performed on other genes

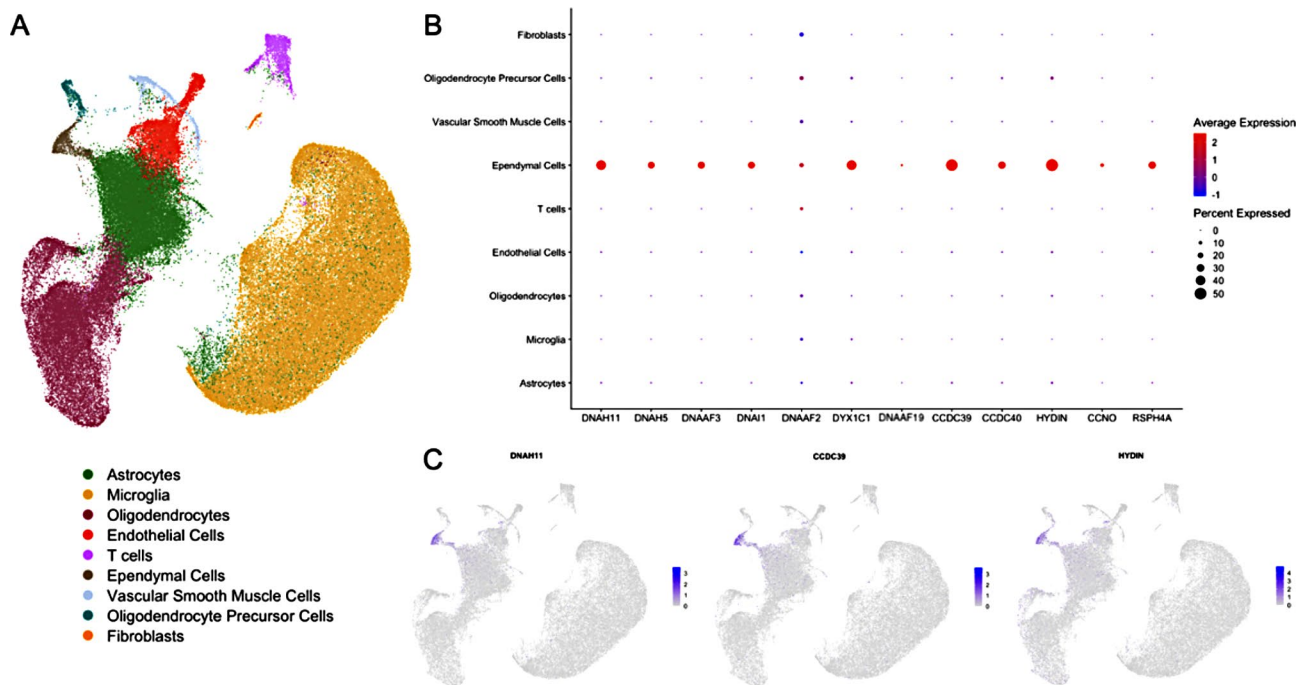


Fig. 1 PCD-associated genes are specifically expressed in brain ependymal cells. **(A)** UMAP of cell types captured from sequencing of 13 periventricular human datasets from 7 patients. The ependymal cell cluster is identified by a brown colour. **(B)** Dot plot of PCD gene expression in all periventricular cell types (fibroblasts, oligodendrocyte precursor cells, vascular smooth muscle cells, ependymal cells, T cells, endothelial cells, oligodendrocytes, microglia and astrocytes) indicating that PCD genes are specifically expressed in ependymal cells ($p < 0.0001$). Average expression values are denoted by a colour scale, with blue indicating low expression and red indicating high expression. Dot size is representative of the percent of cells expressing the gene. **(C)** Feature plots demonstrating specific expression of three representative PCD-associated genes in ependymal cells: *DNAH11*, *CCDC39* and *HYDIN*. Colour indicates gene expression level, with grey indicating low expression and blue indicating high expression

implicated in hydrocephalus. For each PCD case, two control scans were obtained from sex and age-matched (within 6 months) trauma patients who lacked radiologic head injuries. Two trauma control scans were used twice due to limited availability of age and sex matched control scans. Further clinical information on control scan patients, including presence of neuropsychiatric illness, was unavailable. As differing clinical imaging protocols were employed between PCD patients and controls, some findings may have been differentially altered, including image quality, angling of the head, and axial slice thickness. To ensure accurate comparison despite protocol differences, images were manually reviewed, and only scans capturing the lateral ventricles adequately for our measurement protocols were included. Angling of the head was addressed by normalizing measurements to skull size, which scales with angling, and by following established practices for the Evans index, which is measured using the largest diameter of the frontal horns and is captured at any imaging angle. Differences in axial slice thickness were negligible in the context of measuring gross structures spanning many slices.

We compared scans from PCD cases to controls on two measurements calculated using Bee DICOM Viewer software: the normalized ventricular area and the Evans

index (Fig. 2A-D). For the normalized ventricular area, lateral ventricles were manually traced on the single axial slice where they appeared the largest (tracing examples shown in Fig. 2C-D). If there was doubt regarding which axial slice displayed the largest axial area, measurements were taken on multiple adjacent axial slices. Bee DICOM Viewer automatically calculated the area within the traced limits, which was recorded as the largest axial area. Head circumference was measured by manually tracing the outline of the head on a single axial CT image slice above the ears. Normalized ventricular area was calculated as the ratio of the largest axial area of the lateral ventricles and the head circumference. The Evans index, a validated clinical measurement for the diagnosis of hydrocephalus [23], was calculated using the same approach as above, where the width of the frontal horns and the internal diameter of the skull were measured manually on the same axial slice and their ratio was recorded as the Evans index (measurement examples shown in Fig. 2A-B). Scans for patients over age 40 were scored for atrophy using the global cortical atrophy (GCA) scale and the medial temporal atrophy score (MTA). Clinical charts of PCD cases were reviewed for neurologic or psychiatric illness. Normalized ventricular areas and Evans index measurements were compared

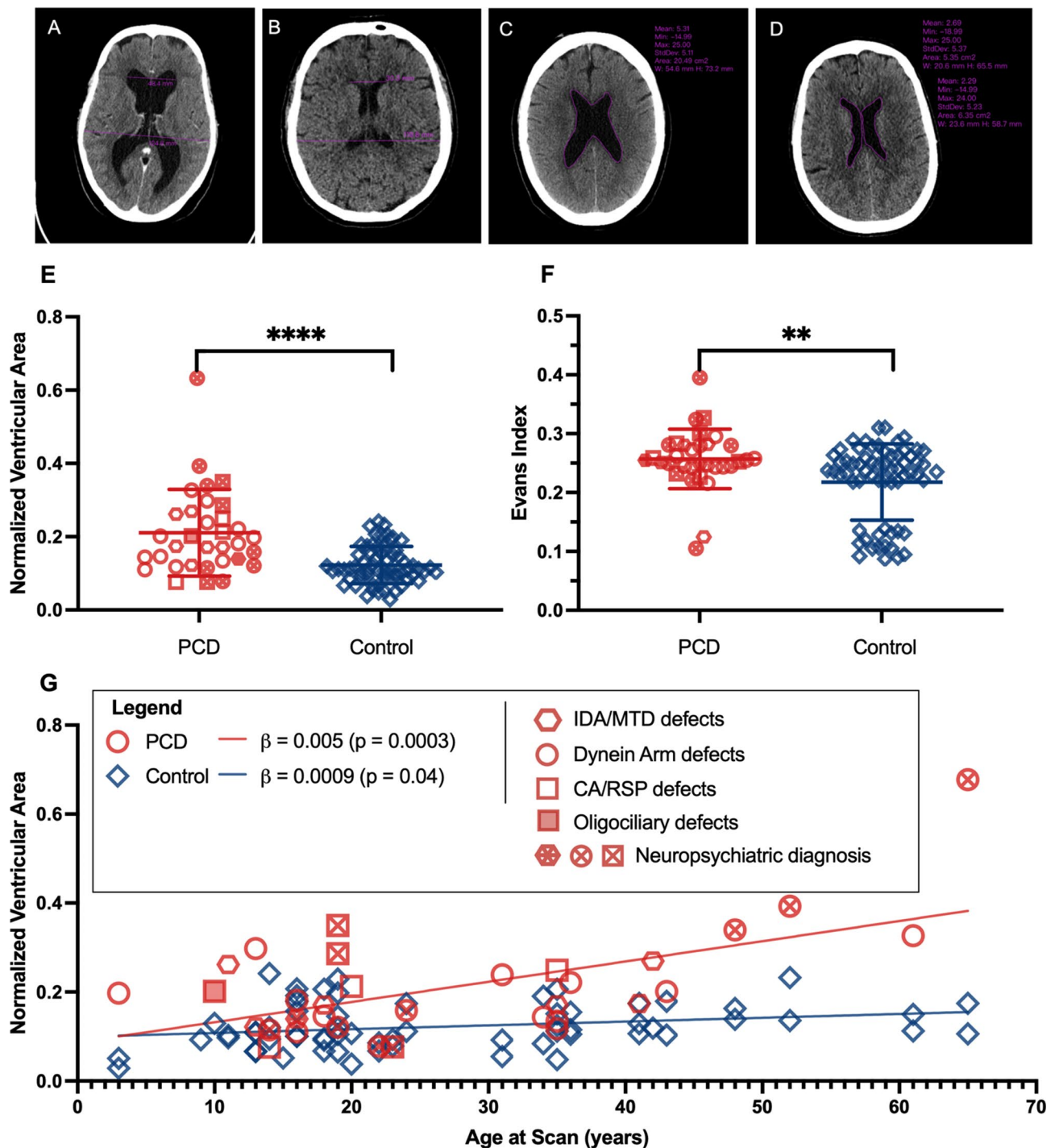


Fig. 2 Normalized ventricular area and Evans index are larger in PCD than control groups. **(A)** Axial slice of the head CT from a patient with PCD from *DNAH5* variants with Evans index measurement - ratio of the maximum width of the frontal horns of the lateral ventricles and the maximal internal diameter of the skull at the same level. **(B)** Axial slice of head CT from corresponding age and sex matched control for the patient in **(A)** with Evans index measurement. **(C)** Axial slice of head CT from patient with PCD from *DNAH11* variants, with measurement of ventricular area. **(D)** Axial slice of head CT from corresponding age and sex matched control for patient in **(C)** with measurement of ventricular area. **(E)** Mean normalized ventricular area is significantly larger in patients with PCD ($0.21 \pm \text{SD}0.12$) than in the Control group ($0.12 \pm \text{SD}0.05$), *****p* < 0.0001. **(F)** Mean Evans index is significantly larger in patients with PCD ($0.26 \pm \text{SD}0.05$) than in the Control group ($0.22 \pm \text{SD}0.06$), ***p* < 0.01. **(G)** Normalized ventricular area plotted against age shows that ventricle size increases significantly more with advancing with age in patients with PCD ($\beta = 0.005$, *p* < 0.001) than in controls ($\beta = 0.0009$, *p* < 0.05).

between PCD and control scans. PCD cases were also grouped according to class of genetic defect for subgroup analysis: (1) Dynein arm defects, (2) IDA/MTD defects, or (3) Oligocilia/CA/RSP defects. Rank-sum tests on yes and no categories were used to compare normalized ventricular area and Evans index in the PCD group with the control group. Multivariate logistic regressions of normalized ventricular area and Evans index were performed for the PCD group with reference to the control group, and within PCD genetic subgroups (IDA/MTD and oligocilia/CA/RSP group with reference to the Dynein arm defects group). Finally, multivariate logistic regressions of normalized ventricular area and Evans index were performed on neuropsychiatric diagnosis (yes/no) within the PCD group. All models were adjusted for age and sex.

Results

Expression levels of genes that are commonly mutated in PCD were evaluated in a human ventricular/periventricular single cell RNA sequencing dataset to determine whether expression was specific to brain ependymal cells (Fig. 1A). We were able to capture all but two of our PCD cohort's genes in our dataset (DNAAF11/LRCC6, DNAAF17/CFAP300), both of which corresponded to one PCD patient. There was considerable variation for all PCD-associated genes assessed, including in the percentage of ependymal cells and the average expression values per ependymal cell that expressed each gene (Fig. 1C). Even so, PCD-associated genes were expressed specifically ($p < 0.0001$) in human brain ependymal cells compared to other periventricular cell types captured in our samples (fibroblasts, oligodendrocyte precursor cells, vascular smooth muscle cells, immune cells, endothelial cells, oligodendrocytes, microglia and astrocytes) (Fig. 1B and C). Even for genes where the percentage of cells expressing that gene was relatively small (CCDC103/DNAAF19, DNAAF2, CCNO), the average expression of the gene in ependymal cells was significantly higher than in other periventricular cell types (Fig. 1B).

Clinical CT scans were available for 47 patients with confirmed PCD, but only 33 scans (mean age $27.3 \pm$ SD 15.2 years, 36% male) captured enough of the ventricles for full analysis. These were compared to 64 age and sex matched trauma control scans. Patients with PCD had a larger mean normalized ventricular area (PCD $0.21 \pm$ SD 0.12, control $0.12 \pm$ SD 0.05, $p < 0.0001$) and Evans index (PCD $0.26 \pm$ SD 0.05, control $0.22 \pm$ SD 0.06, $p < 0.01$) compared to controls (Fig. 2A-E, Supplement Table 2). With logistic regression, the odds ratios for normalized ventricular area and Evans index were 1.202 (95% CI: 1.10–1.31) and 1.139 (95% CI: 1.04–1.25) respectively, indicating that individuals with larger cerebral ventricles were more likely to belong to the PCD group than the control group (Table 1). Three patients in the PCD

group had an Evans index above the cut-off (0.31) for a clinical diagnosis of ventriculomegaly [23]. Shunt insertion was not necessary for any of the affected individuals. A bimodal distribution in Evans index was noted in control patients (Fig. 2F) which could not be attributed to differences in age, sex, image quality, or patient positioning given the nature of the measurement. Linear regression revealed that ventricular size increased markedly with age in patients with PCD ($\beta = 0.005$, $p < 0.0005$) but remained relatively constant in controls ($\beta = 0.0009$, $p < 0.05$) (Fig. 2G). There was no significant brain atrophy in PCD patients > 40 years old compared with controls (Supplementary Table 3). Only one patient, a 65-year-old female with DNAH5 variants (patient ID: PCD11), had signs of more significant brain atrophy than their controls, with an MTA score of 2. This patient also had significant visual disturbances, which may have resulted from optic neuritis associated with prolonged ethambutol use during therapy for an atypical mycobacterium respiratory infection. Intracranial and intraocular pressure were not known in this patient at the time of this study.

Computed tomography scans from patients with PCD were categorized into three genetic subgroups depending on the PCD gene affected: (1) IDA/MTD defects ($n = 6$ total; $n = 3$ CCDC39, $n = 3$ CCDC40), (2) Dynein arm defects ($n = 20$ total; $n = 8$ DNAH11, $n = 4$ DNAH5, $n = 2$ DNAAF3, $n = 1$ for each of DNAIL1, DNAAF2, DNAAF4, DNAAF11, DNAAF17, DNAAF19), or (3) Oligocilia/CA/RSP ($n = 7$ total; $n = 1$ CCNO, $n = 5$ HYDIN, $n = 1$ RSPH4A). Normalized ventricular area and Evans index were similar across genetic subgroups compared to controls and within the subgroups when we compared all PCD categories to the dynein arm defect category (used as our reference group given this group encompassed the most PCD patients).

A diagnosis of neurologic or psychiatric illness was present in 9 of 23 (39%) adults with PCD (with only one patient being purely a neurologic diagnosis). This is elevated over the 12.5% population prevalence of neuropsychiatric illness per the World Health Organization [24]. Diagnoses included depression, dyslexia, schizophrenia, anxiety, migraines, leg weakness/paresthesia, and vision loss. Depression was the most common diagnosis in 36% of adults (Table 2). Pediatric patients with PCD had less neuropsychiatric diagnoses, with 2 out of 10 patients (20%) affected mainly by attention deficit/hyperactivity disorder. Normalized ventricular area and Evans index did not correlate with the presence of a neuropsychiatric disorder ($p = 0.2$ and $p = 0.4$, respectively).

Table 1 Descriptive statistics and logistic regression of normalized ventricular area and Evans index on multiple outcomes^a

	PCD group (n = 33)		Control group (n = 64)		p-value ^b
	N	% of Total	N	% of Total	
Male	12	36.4	24	37.5	0.9126
Female	21	63.6	40	62.5	
	Mean	SD	Mean	SD	p-value ^c
Age at Scan (years)	27.30	15.22	27.06	15.27	0.9331
Head Circumference (cm)	53.39	2.53	54.48	2.49	0.0522
Normalized Ventricular Area ^g	0.21	0.12	0.12	0.05	< 0.0001
Evans Index ^h	0.26	0.05	0.22	0.06	0.0056

	Normalized ventricular area ^d			Evans index ^e		
	Odds ratio	95% CI	p-value	Odds ratio	95% CI	p-value
PCD Group (n = 33)	1.202	(1.10–1.31)	< 0.0001	1.139	(1.04–1.25)	0.0072
Genetic subgroup^f						
Dynein Arm defects (n = 20) ^g	1.000			1.000		
IDA/MTD defects (n = 6) ^h	0.988	(0.89–1.10)	0.8192	0.956	(0.79–1.16)	0.6480
Oligocilia/CA/RSP defects (n = 7) ⁱ	1.084	(0.96–1.22)	0.1897	1.190	(0.88–1.60)	0.2535
Neuropsychiatric diagnosis	1.062	(0.97–1.16)	0.1764	1.086	(0.90–1.32)	0.4036

^aMultivariate models adjusted for age and sex^bChi-square/Fischer exact tests on Yes and No and categories^cRank sum test on Yes and No categories^dRatio of ventricular area and head circumference^eRatio of the maximum width of the frontal horns of the lateral ventricles and the maximal internal diameter of the skull at the same level^fIDA = inner dynein arm defect, MTD = microtubule disorganization, CA = central apparatus, RSP = radial spoke defect^gDNAH11 (N = 8), DNAH5 (N = 4), DNAAF3 (N = 2), DNAI1 (N = 1), DNAAF2 (N = 1), DNAAF4 (N = 1), DNAAF11 (LRRC6) (N = 1), DNAAF17 (CFAP300) (N = 1), DNAAF19 (CCDC103) (N = 1)^hCCDC39 (N = 3), CCDC40 (N = 3)ⁱHYDIN (N = 5), CCNO (N = 1), RSPH4A (N = 1)**Table 2** Neurologic and psychiatric diagnoses in participants with PCD

ID	Age	Sex	Genetic subgroup ^a	PCD gene	Neurologic/psychiatric diagnosis
PCD1	14	F	Dynein arm defects	DNAH5	ADHD ^b
PCD2	16	F	IDA/MTD defects	CCDC40	ADD ^c
PCD3	19	M	Oligocilia/CA/RSP defects	HYDIN	ADHD, dyslexia
PCD4	19	M	Dynein arm defects	DNAAF11 (LRRC6)	Autism, developmental delay
PCD5	19	F	Oligocilia/CA/RSP defects	HYDIN	ADD, depression
PCD6	22	F	Dynein arm defect	DNAH5	Schizophrenia
PCD7	23	F	Oligocilia/CA/RSP defects	RSPH4A	ADHD, anxiety, depression
PCD8	24	M	Dynein arm defects	DNAAF2	Depression, migraine headaches
PCD9	48	F	Dynein arm defects	DNAAF3	Depression
PCD10	52	F	Dynein arm defects	DNAH11	Depression
PCD11	65	F	Dynein arm defects	DNAH5	Leg weakness/paresthesias, vision loss ^d

^aIDA = inner dynein arm defect, MTD = microtubule disorganization, CA = central apparatus, RSP = radial spoke defect^bAttention deficit hyperactivity disorder^cAttention deficit disorder^dThis patient received ethambutol, which is known to cause optic neuritis and other visual disturbances

Discussion

PCD is a genetic disorder that impairs motile ciliary function throughout the body. Most PCD-related gene variants cause severe hydrocephalus in murine models, yet in humans, hydrocephalus only arises with variants

in a few, rare oligociliary genotypes related to NOTCH-1 signaling. Our analysis clarifies that, in fact, people with PCD *do*, more generally, have abnormal features of the brain, such as mild ventricular enlargement compared to controls and even frank ventriculomegaly in some cases.

Based on our gene expression data, PCD genes were specifically expressed by ependymal cells. While the causal link between ependymal ciliary dysfunction and ventriculomegaly in humans remains unknown, our data could suggest defects in this glial cell may represent a possible mechanism behind ventriculomegaly in PCD.

Ventricular enlargement in PCD appears to worsen with age, as adults >40 years old generally showed larger differences in normalized ventricular area compared to age-matched controls. Given this, we were curious whether it relates to idiopathic normal pressure hydrocephalus (iNPH), which is also a disease characterised by ventriculomegaly where prevalence increases with age. There are suggestions of cilia-related defects in genome-wide association studies of iNPH [25], including *CFAP43* [26] and *CWH43* [27]. However, no epidemiology studies have suggested an association between PCD and iNPH. Our data includes mostly young patients with PCD, which is a common limitation because well-defined PCD research cohorts have only recently been developed, and the average age of diagnosis is ~6 years [28]. Thus, most PCD research cohorts worldwide are skewed to include younger patients, and with this age bias, researchers may not easily appreciate the ventriculomegaly that appears to worsen with age.

To date, there are no publications broadly linking PCD with neurologic disease. iNPH is classically associated with gait disturbance, cognitive impairment, and urinary incontinence in patients >60 years of age [29] – though none of our patients displayed these classic symptoms. Rather, we observed many non-specific neurologic issues and psychiatric manifestations, which have previously been linked to ventriculomegaly and hydrocephalus [30–32]. Among pediatric patients, these were primarily neurodevelopmental disorders (attention deficit/hyperactivity disorders). Interestingly, there have been previous findings of increased amounts of extra axial CSF (enlarged subarachnoid space) in patients with autism [33]. Cerebral ventriculomegaly has also been reported in patients with schizophrenia [34]. It is unclear if the observed increase in neuropsychiatric illness in our PCD cohort was related to pathogenesis driven by ventriculomegaly or other factors such as psychosocial stress stemming from having a chronic respiratory disease. One recent psychological screening of patients with PCD showed 30–40% had depression or anxiety, consistent with our findings [35]. Further study of CNS issues in larger PCD patient cohorts, including in-depth neuropsychiatric testing/questionnaires and longitudinal functional brain imaging, may help to determine how ventriculomegaly is associated with neuropsychiatric outcomes in this patient population.

Genotype-phenotype correlation studies in PCD have consistently shown that IDA/MTD defects or biallelic

variants in corresponding *CCDC39* or *CCDC40* genes result in severe respiratory and nutritional outcomes compared to PCD caused by dynein arm defects [36]. This trend was not seen in the ventricular effects of our PCD cohort, as the three genetic subtype groups, including IDA/MTD defects, have similar measures of ventricle size. In other PCD genotypes affected by splice variants or hypomorphic changes, respiratory outcomes may be milder [37, 38]. However, our relatively small number of PCD cases did not afford enough power to perform this type of genetic analysis. Perhaps with larger cohorts of PCD patients, including a wide spectrum of genotypes, genotype-phenotype relationships would be apparent.

The discrepancies between ventriculomegaly in humans and rodent models is a current topic of debate, so our findings are timely [39]. Many hypothesize that PCD variants have a devastating impact in smaller animals as ependymal cilia motility is more important in narrower tubes and ventricular systems due to their small size. The fact that ependymal motile cilia do not scale with ventricle size in higher-order animals lends support for this. However, cilia likely have diverse roles in maintaining CNS homeostasis, for example, through local circulation of CSF and exchange with interstitial fluids, distribution and clearance of intracranial solutes, and pre- and post-natal neurologic development [17–19]. It is possible that ventriculomegaly results from ependymal cell dysfunction in humans through a combination of multiple mechanisms that have yet to be explored. Nonetheless, given multiple PCD genotypes in our cohort contributed to the overall effect of ventriculomegaly, it suggests that ependymal cilia defects are a strong contender for driving ventriculomegaly. At the very least, our findings pose the question of why ventriculomegaly is observed in patients with PCD, if not for ependymal ciliary dysfunction.

Interestingly, ventriculomegaly has been reported on prenatal ultrasound in a small number of infants diagnosed with PCD, but their ventriculomegaly *apparently* resolves by the time of birth [40, 41]. The ependymal cell layer begins differentiating in the human brain as early as 21 weeks gestational age (and fully matures by ~7 months of age) [42], so the observed prenatal ventriculomegaly may be a direct result of the absence of functional motile cilia in early embryonic development, but this does not explain why this largely recovers in the early postnatal year. It also does not explain the age-related increase in ventriculomegaly that we observed later in life. Our finding that ventriculomegaly becomes more severe with age could suggest that vasomotor tone and gravity (the main drivers of bulk CSF flow) are able to partially compensate for ciliopathy-related ventricular dilation for most of one's life, but later in life this compensatory mechanism is inadequate. The reason for this is unknown but could arise from accumulation of toxic solutes over time and

alterations in local CSF exchange with interstitial fluid [43, 44].

As with any observational study, a limitation is that clear cause and effect relationships are challenging to draw. Ventricular dilation may be multifactorial and is difficult to investigate in the context of aging or brain atrophy. Our patient scans were investigated for brain atrophy, and we did not observe any major bias in PCD. Only one patient with PCD had an elevated MTA score versus controls, and this was our oldest participant at age 65 (patient ID: PCD11). Thus, changes in overall brain volume do not appear to account for the ventricular enlargement we see in the PCD group. Another possibility is that the chronic oto-sino-pulmonary infections seen in patients with PCD, although outside of the central nervous system, may impact brain function, resulting in processes that contribute to ventriculomegaly and neurological or psychiatric disease. In light of the COVID-19 pandemic, recent studies have shown that respiratory infections can indeed have lasting impacts on brain health [45].

In conclusion, our results implicate PCD in a neurologic disease process on top of its well-studied effects in the respiratory and reproductive systems. We found that patients with PCD have sub-clinical ventriculomegaly which worsens with age and is consistent across PCD genotypes. We showed specific expression of PCD-related genes in ependymal cells, raising the question whether ependymal ciliary dysfunction may contribute to the observed ventriculomegaly in this population. These findings require further validation, particularly at the molecular level, in animal and human models. Finally, given the high prevalence of neuropsychiatric illness in this population, neurologic and psychiatric screening should be considered in patients with PCD.

Supplementary Information

The online version contains supplementary material available at <https://doi.org/10.1186/s12987-024-00614-9>.

Supplementary Material 1

Supplementary Material 2

Supplementary Material 3

Acknowledgements

We thank the patients with PCD whose data was used for this study; Frederic Lamonde, Raman Agnihotram, Biostatistics Consulting Unit of the McGill University Health Center; Debbie Friedman and Tarek Razek, Trauma program at the McGill University Health Centre; Drs Prat & Zandee for access and reanalysis of MAID single cell sequencing data. This work was presented as an abstract at the American Thoracic Society Conference in 2024, San Diego, California, USA.

Author contributions

FE collected data from CT images and conducted analysis on CT image data, prepared Fig. 2; Tables 1, 2, and contributed to writing the manuscript. JA provided patient CT images and demographic information and conducted

chart review for neuropsychiatric diagnoses. AG contributed all single cell RNA sequencing data, prepared Fig. 1 and contributed to writing relevant sections of the manuscript. JM conducted analysis of cerebral atrophy on CT images (Supplementary Table 3). DR, JS and AS contributed to study design and writing of the manuscript. All authors read and approved the final manuscript.

Funding

Funding was provided by the Tanenbaum Open Science Institute (TOSI) at the Montreal Neurological Institute, the McMaster University Undergraduate Medical Education program, and Stem Cell Network. Support for Adam J. Shapiro by The Genetic Disorders of Mucociliary Clearance Consortium (GDMCC) (U54HL096458). The GDMCC is part of the National Center for Advancing Translational Sciences (NCATS) Rare Diseases Clinical Research Network (RDCRN). RDCRN is an initiative of the Office of Rare Diseases Research (ORDR) funded through a collaboration between NCATS and National Heart, Lung, and Blood Institute (NHLBI).

Data availability

Supporting data is provided in supplementary materials.

Declarations

Ethics approval and consent to participate

Ethical approval and consent were obtained from the Research Ethics Boards of the Montreal Neurological Institute and the McGill University Health Centre (protocol approval number 2023–9159).

Consent for publication

Not applicable.

Competing interests

The authors declare no competing interests.

Received: 5 October 2024 / Accepted: 20 December 2024

Published online: 31 January 2025

References

1. Hannah WB, Seifert BA, Truty R, et al. The global prevalence and ethnic heterogeneity of primary ciliary dyskinesia gene variants: a genetic database analysis. *Lancet Respir Med*. 2022;10(5):459–68. [https://doi.org/10.1016/S2213-2600\(21\)00453-7](https://doi.org/10.1016/S2213-2600(21)00453-7).
2. Zariwala MA, Knowles MR, Leigh MW. Primary ciliary Dyskinesia. In: Adam MP, Feldman J, Mirzaa GM, et al. editors. *GeneReviews*®. Volume 24. Seattle (WA): University of Washington, Seattle; 2007.
3. Deng S, Gan L, Liu C, et al. Roles of Ependymal Cells in the Physiology and Pathology of the Central Nervous System. *Aging and disease*. Published Online January. 2022;1. <https://doi.org/10.14336/ad.2022.0826-1>.
4. Lee L. Riding the wave of ependymal cilia: genetic susceptibility to hydrocephalus in primary ciliary dyskinesia. *J Neurosci Res*. 2013;91(9):1117–32. <https://doi.org/10.1002/jnr.23238>.
5. Shimizu A, Koto M. Ultrastructure and movement of the ependymal and tracheal cilia in congenitally hydrocephalic WIC-Hyd rats. *Child's Nerv Syst*. 1992;8(1):25–32. <https://doi.org/10.1007/bf00316558>.
6. Banizs B, Pike MM, Millican CL, et al. Dysfunctional cilia lead to altered ependyma and choroid plexus function, and result in the formation of hydrocephalus. *Development*. 2005;132(23):5329–39. <https://doi.org/10.1242/dev.02153>.
7. Ibanez-Tallon I. Loss of function of axonemal dynein Mdnah5 causes primary ciliary dyskinesia and hydrocephalus. *Hum Mol Genet*. 2002;11(6):715–21. <https://doi.org/10.1093/hmg/11.6.715>.
8. Borit A, Sidman RL. New mutant mouse with communicating hydrocephalus and secondary aqueductal stenosis. *Acta Neuropathol*. 1972;21(4):316–31. <https://doi.org/10.1007/bf00685139>.
9. Davy BE, Robinson ML. Congenital hydrocephalus in hy3 mice is caused by a frameshift mutation in Hydin, a large novel gene. *Hum Mol Genet*. 2003;12(10):1163–70. <https://doi.org/10.1093/hmg/ddg122>.
10. Olbrich H, Schmidts M, Werner C, et al. Recessive HYDIN mutations cause primary ciliary dyskinesia without randomization of left-right body asymmetry.

- Am J Hum Genet. 2012;91(4):672–84. <https://doi.org/10.1016/j.ajhg.2012.08.016>.
11. Raidt J, Riepenhausen S, Pennekamp P, et al. Analyses of 1236 genotyped primary ciliary dyskinesia individuals identify regional clusters of distinct DNA variants and significant genotype-phenotype correlations. *Eur Respir J*. 2024;64(2):2301769. <https://doi.org/10.1183/13993003.01769-2023>.
 12. Leigh MW, Ferkol TW, Davis SD, et al. Clinical features and associated likelihood of primary ciliary dyskinesia in children and adolescents. *Ann Am Thorac Soc*. 2016;13(8):1305–13. <https://doi.org/10.1513/AnnalsATS.201511-748OC>.
 13. Davis SD, Ferkol TW, Rosenfeld M, et al. Clinical features of childhood primary ciliary dyskinesia by genotype and ultrastructural phenotype. *Am J Respir Crit Care Med*. 2015;191(3):316–24. <https://doi.org/10.1164/rccm.201409-1672OC>.
 14. Amirav I, et al. Systematic analysis of CCNO variants in a defined population: implications for clinical phenotype and differential diagnosis. *Hum Mutat*. 2016;37(4):396–405. <https://doi.org/10.1002/humu.22963>.
 15. Wallmeier J, et al. De novo mutations in FOXJ1 result in a motile ciliopathy with hydrocephalus and randomization of left/right body asymmetry. *Am J Hum Genet*. 2019;105(5):1030–9. <https://doi.org/10.1016/j.ajhg.2019.09.020>.
 16. Robson EA, Dixon L, Causon L, et al. Hydrocephalus and diffuse choroid plexus hyperplasia in primary ciliary dyskinesia-related MCIDAS mutation. *Neurol Genet*. 2020;6(4):e482. <https://doi.org/10.1212/nxg.0000000000000482>.
 17. Sakamoto K, Nakajima M, Kawamura K, et al. Ependymal ciliary motion and their role in congenital hydrocephalus. *Child's Nerv Syst*. 2021;37(11):3355–64. <https://doi.org/10.1007/s00381-021-05194-9>.
 18. Groh AMR, Song YL, Tea F, et al. Multiciliated ependymal cells: an update on biology and pathology in the adult brain. *Acta Neuropathol*. 2024;148(1). <https://doi.org/10.1007/s00401-024-02784-0>.
 19. Groh AMR, Hodgson L, Bzdok D, Stratton JA. Follow the CSF flow: probing multiciliated ependymal cells in brain pathology. *Trends Mol Med*. 2024. <https://doi.org/10.1016/j.molmed.2024.10.007>.
 20. Chen R, et al. Single-cell RNA-Seq reveals hypothalamic cell diversity. *Cell Rep*. 2018;18:3227–41.
 21. MacDonald A, et al. Single cell transcriptomics of Ependymal cells across Age, Region and Species reveals Cilia-Related and Metal Ion Regulatory Roles as Major conserved Ependymal Cell functions. *Front Cell Neurosci*. 2021;15:703951.
 22. Zariwala MA, Knowles MR, Leigh MW et al. Primary ciliary dyskinesia. In: Adam MP, Feldman J, Mirzaa GM, eds. *GeneReviews*® [Internet]. Seattle, WA: University of Washington, Seattle; 1993–2024. Updated December 5, 2019. Accessed November 23, 2024. <https://www.ncbi.nlm.nih.gov/books/NBK1122/>
 23. Relkin N, Marmarou A, Klinge P, Bergsneider M, Black PM. Diagnosing idiopathic normal-pressure hydrocephalus. *Neurosurgery*. 2005;57(3 Suppl):S4–16. discussion ii–v.
 24. World Health Organization. *Mental Disorders*. Updated June 8, 2022. Accessed April 22, 2024. <https://www.who.int/news-room/fact-sheets/detail/mental-disorders>
 25. Yang HW, Lee S, Berry BC et al. A role for mutations in AK9 and other genes affecting ependymal cells in idiopathic normal pressure hydrocephalus. *Proceedings of the National Academy of Sciences*. 2023;120(51). <https://doi.org/10.1073/pnas.2300681120>
 26. Morimoto Y, Yoshida S, Kinoshita A, et al. Nonsense mutation in CFAP43 causes normal-pressure hydrocephalus with ciliary abnormalities. *Neurology*. 2019;92(20). <https://doi.org/10.1212/wnl.0000000000007505>.
 27. Yang HW, Lee S, Yang D, et al. Deletions in CWH43 cause idiopathic normal pressure hydrocephalus. *EMBO Mol Med*. 2021;13(3). <https://doi.org/10.15252/emmm.202013249>.
 28. Kuehni CE, Frischer T, Strippoli MP, et al. Factors influencing age at diagnosis of primary ciliary dyskinesia in European children. *Eur Respir J*. 2010;36(6):1248–58. <https://doi.org/10.1183/09031936.00001010>.
 29. Xiao H, Hu F, Ding J, Ye Z. Cognitive impairment in idiopathic normal pressure hydrocephalus [published correction appears in *Neurosci Bull*. 2022]. *Neurosci Bull*. 2022;38(9):1085–96. <https://doi.org/10.1007/s12264-022-00873-2>.
 30. Alao AO, Naprawa SA. Psychiatric complications of hydrocephalus. *Int J Psychiatry Med*. 2001;31:337–40. <https://doi.org/10.2190/8KLO-HGB3-XN2P-5Y8K>.
 31. Kito Y, Kazui H, Kubo Y, et al. Neuropsychiatric symptoms in patients with idiopathic normal pressure hydrocephalus. *Behav Neurol*. 2009;21:165–74. <https://doi.org/10.3233/BEN-2009-0232>.
 32. Oliveira MFD O, JRMD, Rotta JM, Pinto F. Psychiatric symptoms are present in most of the patients with idiopathic normal pressure hydrocephalus. *Arq Neuropsiquiatr*. 2014;72(6):435–8. <https://doi.org/10.1590/0004-282X20140047>.
 33. Shen MD, Nordahl CW, Li DD, et al. Extra-axial cerebrospinal fluid in high-risk and normal-risk children with autism aged 2–4 years: a case-control study. *Lancet Psychiatry*. 2018;5(11):895–904. [https://doi.org/10.1016/s2215-0366\(18\)30294-3](https://doi.org/10.1016/s2215-0366(18)30294-3).
 34. del RE EC, Konishi J, Bouix S, et al. Enlarged lateral ventricles inversely correlate with reduced corpus callosum central volume in first episode schizophrenia: association with functional measures. *Brain Imaging Behav*. 2015;10(4):1264–73. <https://doi.org/10.1007/s11682-015-9493-2>.
 35. Graziano S, Ullmann N, Rusciano R, et al. Comparison of mental health in individuals with primary ciliary dyskinesia, cystic fibrosis, and parent caregivers. *Respir Med*. 2023;207:107095. <https://doi.org/10.1016/j.rmed.2022.107095>.
 36. Davis SD, Rosenfeld M, Lee HS, et al. Primary ciliary Dyskinesia: Longitudinal Study of Lung Disease by Ultrastructure Defect and Genotype. *Am J Respir Crit Care Med*. 2019;199(2):190–8. <https://doi.org/10.1164/rccm.201803-0548OC>.
 37. Shoemark A, Moya E, Hirst RA, et al. High prevalence of CCDC103 p.His154Pro mutation causing primary ciliary dyskinesia disrupts protein oligomerization and is associated with normal diagnostic investigations. *Thorax*. 2018;73(2):157–66. <https://doi.org/10.1136/thoraxjnl-2017-209999>.
 38. Ostrowski LE, Yin W, Smith AJ, et al. Expression of a truncated form of ODAD1 Associated with an unusually mild primary ciliary Dyskinesia phenotype. *Int J Mol Sci*. 2022;23(3):1753. <https://doi.org/10.3390/ijms23031753>. Published 2022 Feb 3.
 39. Duy PQ, Greenberg ABW, Butler WE, Kahle KT. Rethinking the cilia hypothesis of hydrocephalus. *Neurobiol Dis*. 2022;175:105913. <https://doi.org/10.1016/j.nbd.2022.105913>.
 40. Wessels MW, den Hollander NS, Willems PJ. Mild fetal cerebral ventriculomegaly as a prenatal sonographic marker for Kartagener syndrome. *Prenat Diagn*. 2003;23(3):239–42. <https://doi.org/10.1002/pd.551>.
 41. Mapala L, Kumar M, Canakis AM, Hailu E, Kopel LS, Shapiro AJ. Recognizing clinical features of primary ciliary dyskinesia in the perinatal period. *J Perinatol* Published Online July. 2024;24. <https://doi.org/10.1038/s41372-024-02068-1>.
 42. Coletti AM, Singh D, Kumar S et al. Characterization of the ventricular-subventricular stem cell niche during human brain development. *Development*. 2018;145(20):dev170100. Published 2018 Oct 26. <https://doi.org/10.1242/dev.170100>
 43. Yoshida H, Ishida S, Yamamoto T, et al. Effect of cilia-induced surface velocity on cerebrospinal fluid exchange in the lateral ventricles. *J R Soc Interface*. 2022;19(193):20220321. <https://doi.org/10.1098/rsif.2022.0321>.
 44. Jiménez AJ, Domínguez-Pinos MD, Guerra MM, Fernández-Llebreg P, Pérez-Figares JM. Structure and function of the ependymal barrier and diseases associated with ependyma disruption. *Tissue Barriers*. 2014;2:e28426. Published 2014 Mar 19. <https://doi.org/10.4161/tisb.28426>
 45. Ramasamy A, Wang C, Brode WM, Verdusco-Gutierrez M, Melamed E. Immunologic and autoimmune-related sequelae of severe Acute Respiratory Syndrome Coronavirus 2 infection. *Phys Med Rehabil Clin North Am*. 2023;34(3):623–42. <https://doi.org/10.1016/j.pmr.2023.04.004>.

Publisher's note

Springer Nature remains neutral with regard to jurisdictional claims in published maps and institutional affiliations.